Effects of interfacial roughness on the magnetoresistance of magnetic metallic multilayers

Randolph Q. Hood and L. M. Falicov
Department of Physics, University of California, Berkeley, California 94720
and Materials Sciences Division, Lawrence Berkeley Laboratory, University of California, Berkeley, California 94720

D. R. Penn
Electron Physics Group, National Institute of Standards and Technology, Gaithersburg, Maryland 20899
(Received 3 August 1993)

The Boltzmann equation is solved for a system consisting of a ferromagnetic–normal-metallic multilayer. The in-plane magnetoresistance of Fe/Cr and Fe/Cu superlattices is calculated for (1) varying interfacial geometric random roughness with no lateral coherence, (2) correlated (quasiperiodic) roughness, and (3) varying chemical composition of the interfaces. The interplay between these three aspects of the interfaces may enhance or suppress the magnetoresistance, depending on whether it increases or decreases the asymmetry in the spin-dependent scattering of the conduction electrons. Properties of the interfaces relevant to the giant negative magnetoresistance are discussed.

I. INTRODUCTION

Multilayers composed of alternating layers of ferromagnetic (F) metals separated by normal-metallic spacer (S) layers, in which the magnetic moments of the neighboring F layers are arranged in an antiparallel configuration to each other, show a drop in resistivity under the application of an external magnetic field; this drop occurs as the field aligns the magnetic moments of the F layers parallel to each other. This negative magnetoresistance (MR) has been observed in various sandwiches[1–7] and superlattices,[8–12] such as NiFe/Cu/NiFe, NiFe/Ag/NiFe, $(Fe/Cr)_n$, $(Co/Cu)_n$, $(Fe/Cu)_n$, and $(Co/Ru)_n$ to name just a few. In some cases the MR is large,[8,10] as in $(Fe/Cr)_n$ and $(Co/Cu)_n$. Currently[10] the largest MR observed at room temperature is in the $(Co/Cu)_n$ multilayer where the MR defined as $\Delta\rho/\rho=[R(0)-R(H_{sat})]/R(H_{sat})$, is as large as 65% for a saturating field H_{sat} as small as 10 kOe. Systems with a MR larger than 20% are said to exhibit a giant magnetoresistance (GMR) and could be very useful for applications in microelectronic devices.

Experimental[13–15] investigations seeking the origin of the GMR have found that the interfaces in the multilayers play a key role. Depositing ultrathin layers of elements (V, Mn, Ge, Ir, and Al) at the Fe-Cr interfaces Baumgart *et al.*[13] found that the MR changed in a manner which correlated with the ratio of spin-up and spin-down resistivities arising from spin-dependent impurity scattering of these elements when alloyed with Fe. Parkin[14] found that the addition of thin Co layers at the interfaces of NiFe-Cu multilayers enhanced the MR. The MR increased monotonically as the Co layer increased to 4 Å, then became insensitive to the thickness of the Co layer with a MR similar to that of $(Co/Cu)_n$ despite the presence of NiFe layers sandwiched between the thin Co layers. Fullerton *et al.*[15] found that a systematic increase in the interfacial roughness at Fe-Cr interfaces enhanced the MR.

Most of the theoretical approaches[16–20] assume that the current is carried by two conduction-electron channels, associated with spin-up and spin-down electrons. Sizable values of the MR are obtained when total scattering rates for the spin channels are very different both between themselves and in the two magnetic configurations. These theories[16–19] predict a GMR when the main spin-dependent scattering mechanism is localized around the interfaces and a smaller MR when the predominant spin-dependent scattering occurs within the bulk of the layers.

A precise description of the character of the interfaces and the resulting spin-dependent scattering mechanisms are currently unavailable either from experiment or from theory. There are several possibilities, which depend on the growth conditions and the materials used during fabrication. Interdiffusion may be present and intermix the elements within a region around each of the interfaces. By contrast there may be regions, laterally along the interfaces, with little interdiffusion but with variations in thickness, i.e., geometrical roughness. The variations in thickness may vary in a random manner with little lateral coherence, or there may be steps and terraces with considerable correlations. In addition there may be chemical impurities at the interfaces that may have been introduced, intentionally or unintentionally. In principle both the position and the type of atoms present at the interfaces can influence the spin-dependent scattering of the conduction electrons.

In this contribution we present an extension of a previous semiclassical (Boltzmann) approach,[16] hereafter referred to as BA, that looks at how particular changes in the structure and the chemical composition of the interfaces influence the interfacial spin-dependent scattering mechanism and, more importantly, the MR. Specifically we consider how the MR is affected by (1) variations in the size of the geometrical roughness, the mean-square deviation of the surfaces from being atomically flat, with no lateral coherence, (2) the presence of correlated (quasiperiodic) roughness, and (3) the chemical composition of the interface. With few exceptions, the simple rule that

0163-1829/94/49(1)/368(10)/$06.00

emerged in BA does not change. That is, in order to have a GMR, it is advantageous to have a large asymmetrical spin-dependent interfacial scattering mechanism, with one spin component largely scattered diffusely, and the other mainly scattered coherently by the potentials. What emerges from this study is an understanding of how different qualities of the interfaces leads to asymmetrical spin-dependent scattering. In some cases the interplay of the different aspects of the interfaces we mention above may enhance the asymmetrical nature of the interfacial spin-dependent scattering and hence the MR; in other cases it may decrease the asymmetry and correspondingly suppress the MR.

As in BA—an extension of the Fuchs-Sondheimer theory[21,22] and Camley and Barnas's approach[17,18] to multilayers—we use a Stoner description[23] of the itinerant F layers; there are different potentials for the majority and minority spins. Band-structure and electron-density effects are included by means of constant metal- and spin-dependent potentials, and an isotropic effective mass for each spin in each layer. As an electron traverses an F-S interface the potential difference between the layers causes it to be partially reflected, with a probability R, and partially transmitted (refracted) into the other layer, with probability T. The coefficients R and T are determined by quantum-mechanical matching of the wave functions at the interface, and found in general to depend on the Fermi velocity, the orientation of the spin, and the angle of incidence. In addition a single spin-dependent parameter S is introduced at each interface to characterize the fraction of electrons which are coherently scattered by the potential. The remainder, $(1-S)$, is assumed to be diffusely scattered back to the equilibrium distribution. In BA it was assumed that S was independent of the angle and direction of incidence. It represents the averaged effects of any spin-dependent interfacial scattering mechanisms present at the interfaces not caused by the potential difference. In other words, it represented the average effect of the structural and chemical imperfections at the interfaces. In the current contribution we show that it is possible to quantify specific information about the interfaces by allowing S to depend more generally on the angle and direction of incidence, and the spin orientation.

In Sec. II we present a summary of the model. Section III contains a discussion of the interfacial scattering parameters S. In Sec. IV results are presented for various interfaces in $(\mathrm{Fe/Cr})_n$ and $(\mathrm{Fe/Cu})_n$ multilayers. Section V contains the conclusions.

II. THE MODEL

The in-plane conductivity is calculated for a trilayer with periodic boundary conditions at the outer surfaces—to be described shortly—so as to represent a superlattice. Both the current J and the time-independent electric field E are in the $\hat{\mathbf{x}}$ direction. The $\hat{\mathbf{z}}$ axis is taken to be normal to the layers. The trilayer unit consists of three flat layers (labeled 1, 2, and 3) of infinite extent in the $\hat{\mathbf{x}}$ and the $\hat{\mathbf{y}}$ directions of thicknesses d_1, d_2, and d_3. The structures investigated have identical F materials in layers 1 and 3 and an S normal metal in layer 2.

For a given trilayer the conductivity is calculated for both the parallel ($\sigma\uparrow\uparrow$, for large applied magnetic field) and antiparallel ($\sigma\uparrow\downarrow$, no magnetic field) arrangements of the F layers 1 and 3. The magnetoresistance $(\Delta\rho/\rho)$, is defined by

$$\frac{\Delta\rho}{\rho}\equiv\frac{\rho\uparrow\downarrow-\rho\uparrow\uparrow}{\rho\uparrow\downarrow}=\frac{\sigma\uparrow\uparrow-\sigma\uparrow\downarrow}{\sigma\uparrow\uparrow}\ , \tag{1}$$

where $\rho_{\mu\nu}=(\sigma_{\mu\nu})^{-1}$. Note that this quantity varies between zero and one (or 0 and 100 %) whenever the resistance decreases upon the application of an external magnetic field.

The conductivity for both alignments is obtained by adding the contributions of the spin-up and the spin-down electrons, calculated separately. This is the two-current model,[24] which provides a good description of electron transport in magnetic $3d$ metals. Spin-flip processes, which mix the two currents, are neglected. It is known that their effect is small at low temperatures.[24]

The electrons involved in transport are regarded as free-electron-like with spherical Fermi surfaces. Within each layer the electrons move in a constant potential $V_{i\sigma}$, which depends on the particular layer i and the spin σ of the electron.

The electron distribution function within each layer i and for each spin σ is written in the form

$$f_{i\sigma}(\mathbf{v},z)=f^0_{i\sigma}(\mathbf{v})+g_{i\sigma}(\mathbf{v},z)\ , \tag{2}$$

which is independent of x and y by symmetry. In (2), the first term $f^0_{i\sigma}(\mathbf{v})$ is the equilibrium distribution in the absence of an electric field and $g_{i\sigma}(\mathbf{v},z)$ is the deviation from that equilibrium in the presence of the electric field. For an electric field of magnitude E in the $\hat{\mathbf{x}}$ direction, the Boltzmann equation in the relaxation time approximation reduces to

$$\frac{\partial g_{i\sigma}}{\partial z}+\frac{g_{i\sigma}}{\tau_{i\sigma}v_z}=\frac{|e|E}{m_{i\sigma}v_z}\frac{\partial f^0_{i\sigma}}{\partial v_x}\ , \tag{3}$$

where $\tau_{i\sigma}$ is the relaxation time in layer i for spin σ, and e is the charge of the electron. The second-order term, proportional to $(E\cdot g_{i\sigma})$, has been discarded since nonlinear effects (deviations from Ohm's law) are neglected. The Lorentz-force term, proportional to $(\mathbf{v}\times\mathbf{H}/c)$, has also been dropped from the Boltzmann equation, since it gives an effect which is orders of magnitude smaller than those considered here.[18]

Because of the boundary conditions it is useful to divide $g_{i\sigma}$ into two parts: $g^+_{i\sigma}(\mathbf{v},z)$ if $v_z\geq 0$ and $g^-_{i\sigma}(\mathbf{v},z)$ if $v_z<0$. The general solution to Eq. (3) takes the form

$$g^{\pm}_{i\sigma}(\mathbf{v},z)=\frac{|e|\tau_{i\sigma}E}{m_{i\sigma}}\frac{\partial f^0(\mathbf{v})}{\partial v_x}\times\left\{1+F^{\pm}_{i\sigma}(\mathbf{v})\exp\left[\mp\frac{z}{\tau_{i\sigma}|v_z|}\right]\right\}\ , \tag{4}$$

where the functional form of $F_{i\sigma}(\mathbf{v})$ is determined by requiring the electron distribution function to satisfy the boundary conditions described below.

At the two outer surfaces of the unit trilayer, the periodic boundary conditions are

$$\begin{aligned} g^{+}_{1\sigma} &= g^{-}_{1\sigma} \quad \text{at } z=0 \ , \\ g^{-}_{3\sigma} &= g^{+}_{3\sigma} \quad \text{at } z=d \ , \end{aligned} \tag{5}$$

where $d=d_1+d_2+d_3$ is the total thickness of the trilayer. These boundary conditions[25] cause the trilayer to be equivalent to a superlattice of the form

$$\cdots |2d_1|d_2|2d_3|d_2|2d_1|d_2|2d_3| \cdots \ .$$

In (5), and in the boundary conditions at the interfaces in (6) below, the explicit functional dependence of the distribution functions $g^{\pm}_{i\sigma}$ has been dropped.

The boundary conditions for the potential (nondiffusive) scattering at the 1-2 and 2-3 interfaces take the form

$$\begin{aligned} g^{-}_{1\sigma} &= S_{12;1;\sigma} R_{12\sigma} g^{+}_{1\sigma} + S_{21;1;\sigma} T_{21\sigma} g^{-}_{2\sigma} \quad \text{at } z=d_1 \ , \\ g^{+}_{2\sigma} &= S_{21;2;\sigma} R_{21\sigma} g^{-}_{2\sigma} + S_{12;2;\sigma} T_{12\sigma} g^{+}_{1\sigma} \quad \text{at } z=d_1 \ , \\ g^{-}_{2\sigma} &= S_{23;2;\sigma} R_{23\sigma} g^{+}_{2\sigma} + S_{32;2;\sigma} T_{32\sigma} g^{-}_{3\sigma} \quad \text{at } z=d_1+d_2 \ , \\ g^{+}_{3\sigma} &= S_{32;3;\sigma} R_{32\sigma} g^{-}_{3\sigma} + S_{23;3;\sigma} T_{23\sigma} g^{+}_{2\sigma} \quad \text{at } z=d_1+d_2 \ . \end{aligned} \tag{6}$$

Here $S_{ij;l;\sigma}$ which vary between zero and one, are factors that indicate the degree of potential scattering at each of the interfaces $i-j$ for a spin σ electron arriving from layer i and being scattered into the layer l. The scattering follows the reflection-refraction laws when $S=1$ and is completely diffusive when $S=0$. The notation used for the transmission T and the reflection R coefficients is the following: $T_{ij\sigma} \equiv$ probability for an electron of spin σ in layer i to be transmitted (refracted) into layer j; $R_{kl\sigma} \equiv$ probability for an electron of spin σ in layer k with a velocity directed towards layer l to be reflected back into layer k. The equations and boundary conditions, as written, satisfy all the necessary conservation laws.

In Sec. III we discuss the functional dependence of the interfacial parameters $S_{ij;l;\sigma}$. The functional dependence of the reflection $R_{ij\sigma}$ and transmission $T_{ij\sigma}$ coefficients was determined by matching the free-electron-like (plane-wave) functions and their derivatives at each interface. The solution to this problem is identical to that encountered in optics for an interface between two media with different indices of refraction. The reflection R and transmission T coefficients take the form

$$\begin{aligned} R_{ij\sigma}(E,\theta) &= \left| \frac{1-h_{ij\sigma}(E,\theta)}{1+h_{ij\sigma}(E,\theta)} \right|^2 \ , \\ T_{ij\sigma}(E,\theta) &= \frac{4\,\mathrm{Re}[h_{ij\sigma}(E,\theta)]}{|1+h_{ij\sigma}(E,\theta)|^2} = 1-R_{ij\sigma}(E,\theta) \ . \end{aligned} \tag{7}$$

Here θ is the angle of incidence, measured with respect to the z axis, of an electron of energy $E=\frac{1}{2}m_{i\sigma}v^2+V_{i\sigma}$ in layer i with spin σ and velocity v moving in a constant potential $V_{i\sigma}$. The scattering is completely elastic, i.e., the energy of the electron is a constant of the motion. The symbol Re means "the real part of"; the function $h_{ij\sigma}(E,\theta)$ has the form

$$h_{ij\sigma}(E,\theta) = \frac{\sqrt{(E-V_{j\sigma})/(E-V_{i\sigma}) - \sin^2\theta}}{\cos\theta} \ . \tag{8}$$

The transmission and reflection coefficients appearing in (6) are related by

$$\begin{aligned} R_{ij\sigma}(E,\theta_i) &= R_{ji\sigma}(E,\theta_j) \ , \\ T_{ij\sigma}(E,\theta_i) &= T_{ji\sigma}d(E,\theta_j) \ , \end{aligned}$$

where

$$\frac{\sin\theta_i}{\sin\theta_j} = \sqrt{(E-V_{j\sigma})/(E-V_{i\sigma})} \ ;$$

this is a consequence of the principle of microscopic (optical) reversibility.

Substitution of Eq. (4) into the boundary conditions, Eqs. (5) and (6), yields unique solutions of $F^{\pm}_{i\sigma}(\mathbf{v})$. The current density along the electric field in each layer i for electrons with spin σ is given by

$$J_{xi\sigma}(z) = -|e| \left[\frac{m_{i\sigma}}{h} \right]^3 \int v_x g_{i\sigma}(\mathbf{v},z) d^3\mathbf{v} \ , \tag{9}$$

where h is Planck's constant.

In order to obtain the MR one requires the effective conductivity, which is found by averaging over the whole film

$$\sigma = \frac{1}{Ed} \sum_{i=1}^{i=3} \sum_{\sigma=\uparrow,\downarrow} \int J_{xi\sigma}(z) dz \ .$$

Details of this integration can be found in BA.

The MR, $(\Delta\rho/\rho)$, is found by calculating independently the conductivities $\sigma\uparrow\downarrow$ and $\sigma\uparrow\uparrow$. There are several parameters necessary to characterize completely a structure. Associated with the electrons in layers 1 and 3 are the minority (denoted using a small subscript m) and the majority (denoted using a capital subscript M) spins with effective masses m_m and m_M, relaxation times τ_m and τ_M, and potentials V_m and V_M. The spin-up and spin-down electrons in layer 2, which is the normal-metal S layer, move in a potential V_S with an effective mass m_S and relaxation time τ_S.

The values of the potentials are determined by treating all of the valence electrons as being in a single free-electron-like band with an isotropic effective mass. The effective mass is, in general, taken to be larger than the electron mass, since the d-like electrons are in narrower bands than the free-electron-like s electrons. Within the ferromagnetic layers 1 and 3, the bands for the minority and the majority spins are shifted by a k-independent exchange potential, yielding two different spin-dependent, constant potentials, V_m and V_M. The value of the exchange splitting is chosen so that the difference in the density of the majority and the minority electrons yields the net magnetic moment of the bulk ferromagnetic material. The present model neglects band-structure effects.

III. INTERFACE PARAMETERS

In this section we discuss the functional form of $S_{ij;l;\sigma}$. The treatment of interfacial scattering in BA described the averaged effects of roughness and the presence of impurities by the two parameters S_M and S_m for the majority and the minority spins, respectively. This can be viewed as a special case that occurs when the function $S_{ij;l;\sigma}$ is independent of the direction and angle of incidence at the interface. Formally

$$S_{F,S;F;M}=S_{F,S;S;M}=S_{S,F;F;M}=S_{S,F;S;M}=S_M \ ,$$
$$S_{F,S;F;m}=S_{F,S;S;m}=S_{S,F;F;m}=S_{S,F;S;m}=S_m \ . \tag{10}$$

When there is little interdiffusion, an interface separating a spacer and a ferromagnetic layer can be described by a function $z=z_{ij}+\zeta(x,y)$, where z is the coordinate normal to the layers and z_{ij} is the average coordinate of the interface, $z_{1,2}=d_1$ or $z_{2,3}=d_1+d_2$. In general the specific form of the function ζ for a given interface is unknown: A statistical description of an interface is appropriate. A common approach[26–29] is to consider ζ as a random variable with a Gaussian distribution

$$w(\zeta)=\frac{1}{\eta\sqrt{2\pi}}e^{-\zeta^2/2\eta}$$

that is independent of position in the (x,y) plane, so that

$$\eta=\sqrt{\langle \zeta(z,y)^2\rangle} \ ,$$

and that the in-plane correlation function between two points in the interface is

$$C\left[|\mathbf{r}_1-\mathbf{r}_2|\right]\equiv\langle \zeta(\mathbf{r}_1)\zeta(\mathbf{r}_2)\rangle/\langle \zeta(\mathbf{r}_1)\rangle^2 = e^{-|\mathbf{r}_1-\mathbf{r}_2|^2/L^2} \ ,$$

where $\mathbf{r}=x_i\hat{\mathbf{x}}+y_i\hat{\mathbf{y}}$ and L is the correlation length. For a finite nonzero L, the boundary conditions, Eq. (6), must be replaced by a set of integral equations, since the diffuse scattering makes a contribution to the current. In the limit as L goes to zero the diffuse scattering no longer contributes to the current, Eq. (6) is valid,[30] and the function $S_{ij;l;\sigma}$ takes the form (see Refs. 26 and 27 for a derivation and discussion):

$$S_{ij;i;\sigma}=S_\sigma \exp[-4\eta^2(k_{i\sigma}\cos\theta_i)^2] \ ;$$
$$S_{ij;j;\sigma}=S_\sigma \exp[-\eta^2(k_{i\sigma}\cos\theta_i-k_{j\sigma}\cos\theta_j)^2] \ . \tag{11}$$

Here $k_{i\sigma}$ is related to the magnitude of the velocity of an electron in layer i with spin σ, given by $k_{i\sigma}=m_{i\sigma}v_{i\sigma}/\hbar$. We have inserted the prefactor S_σ in Eq. (11) to include, in an averaged way, the scattering effects from impurities, interdiffusion, band structure, correlation, etc., caused neither by potential difference at the interface nor by geometrical roughness.[31]

The presence of roughness causes spin-dependent scattering at the interfaces since for electrons at the Fermi energy in the ferromagnetic layers $i=F$, the $k_{i\sigma}$ have magnitudes that depend on the spin σ. From Eq. (11) the diffuse scattering is considerably larger for electrons impinging upon the interface in directions close to the normal. Grazing-angle electrons are less effectively scattered, and they tend to be almost completely internally reflected.

If the surface, on the other hand, has strong lateral correlations, with typical correlation lengths of the order of the Fermi wavelength, quantum-mechanical coherence effects may take place. In particular, the presence of a "periodic" potential that satisfies Bragg's condition is responsible for electron-diffraction phenomena. Roughness at interfaces with strong in-plane spatial correlations and with typical lengths of, say, the Fermi wavelength of the majority-spin electrons, will cause these electrons—which match Bragg's diffraction condition—to be coherently scattered onto the Bragg-peak directions, and removed from the reflected and transmitted beams more efficiently. These Bragg-diffracted electrons do not contribute effectively to the conduction processes. A given "cone" of electrons of a given spin is thus removed, at the interface, from the current-carrying stream.[32] For strongly peaked in-plane correlation lengths this process may affect one spin and not the other.

Bragg's condition follows from the conservation of the electron total energy and crystal momentum in the plane of the interface. An electron with $\mathbf{k}_{i\sigma}$ in layer i, with spin σ, incident on an interface separating the i and j layers is predominantly diffracted into those directions $\mathbf{k}_{l\sigma}$ (where $l=i$ or j) that satisfy[33]

$$|\mathbf{k}_{i\sigma\parallel}|^2+k_{i\sigma\perp}^2=|k_{l\sigma\parallel}|^2+k_{l\sigma\perp}^2+\frac{2\cdot m}{\hbar^2}(V_{l\sigma}-V_{i\sigma}) \ , \tag{12}$$

$$\mathbf{k}_{l\sigma\parallel}=\mathbf{k}_{i\sigma\parallel}+\mathbf{K}_{ij} \ . \tag{13}$$

Here $\mathbf{K}_{ij}$ is any (two-dimensional) reciprocal-lattice vector in the plane of the interface (say the x,y plane) that is related to the real-space quasiperiodic roughness of the (ij) interface. A pictorial representation of Bragg's condition in reciprocal space is shown in Fig. 1. Because of lack of periodicity in the z direction, there is conservation of crystal momentum only in the x,y plane, as stated in (13). The "Bragg spots" (three-dimensional reciprocal-lattice vectors) are in this case "Bragg rods," lines parallel to z (perpendicular to the interface) that pass through each point $\mathbf{K}_{ij}$. In Fig. 1 these rods are drawn along with two hemispheres centered at the origin of $\mathbf{k}_{i\sigma}$. The radius of each hemisphere follows from Eq. (12) and depends on whether the electrons are scattered into layer i (backward scattering) or layer j (forward scattering). Possible $\mathbf{k}_{l\sigma}$ (i.e., those that satisfy the equations above) are drawn with the tail at the center of the two hemispheres and the head at those points where a hemisphere intersects one rod. Two cases, $V_{i\sigma}<V_{j\sigma}$ and $V_{i\sigma}>V_{j\sigma}$ are illustrated in Fig. 1. In both cases shown a reflected R and a transmitted T beam occur. In addition the angle of incidence was chosen in each case such that an additional diffracted beam D just appears. This has the effect of reducing the intensity of the reflected and the transmitted beams. The threshold angle of incidence θ_t, at which a diffracted peak appears is given by

$$|\mathbf{k}_{i\sigma}|\sin(\theta_t)+k_{\max,\sigma}=\kappa_{ij} \ ,$$

where κ_{ij} is the smallest nonzero reciprocal-lattice vector and $k_{\max,\sigma}$ is equal to the maximum value of the magni-

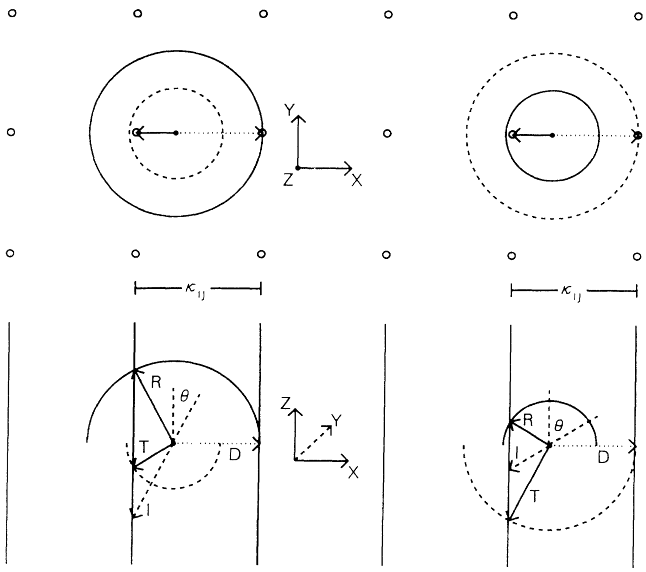

FIG. 1. Illustration of the Bragg condition in reciprocal space for a periodically modulated interface with a minimum nonzero reciprocal-lattice vector κ_{ij} viewed from two different perspectives and for two different cases: on the left side $V_{i\sigma} < V_{j\sigma}$; and on the right side $V_{i\sigma} > V_{j\sigma}$. The perspectives at the top of the figure are in the plane of the interface; the "Bragg rods" are out of the page. Hemispheres of **k** vectors for the two films at the interface, corresponding to an incident $\mathbf{k}_{i\sigma}$, labeled I, with the angle of incident θ are shown. The solid vectors labeled R and T are the reflected and transmitted beams, respectively. The angle θ was chosen in each case to equal the threshold angle. A single grazing-angle additional diffraction peak occurs either in back scattering (left) or in forward scattering (right). The corresponding **k** vectors are shown (dotted vectors), and labeled D in the figure.

tudes of the two vectors $\mathbf{k}_{i\sigma}$ and $\mathbf{k}_{j\sigma}$. In this equation an average was taken over the azimuthal component of $\mathbf{k}_{i\sigma}$, assuming a polycrystalline interface as in most common situations. The removal of electrons from the reflected and the transmitted beams can be taken into account by assuming that in the range of angles, $\theta > \theta_t$ the corresponding functions $S_{ij;l;\sigma}$ are substantially reduced. This can be achieved by multiplying $S_{ij;l;\sigma}$ by a factor $0 \le c_{ij;l;\sigma} \le 1$.

A suitable function, used in the calculations is

$$c_{ij;l;\sigma} = 1, \quad \text{if } \kappa_{ij} > k_{i,\sigma} + k_{\max,\sigma} \; ;$$

$$c_{ij;l;\sigma} = 1, \quad \text{if } \kappa_{ij} \le k_{i,\sigma} + k_{\max,\sigma}$$

and

$$\theta < \sin^{-1}\left[\frac{\kappa_{ij} - k_{\max,\sigma}}{k_{i,\sigma}}\right] ; \tag{14}$$

$$c_{ij;l;\sigma} = (1-\alpha), \quad \text{if } \kappa_{ij} \le k_{i,\sigma} + k_{\max,\sigma}$$

and

$$\theta \ge \sin^{-1}\left[\frac{\kappa_{ij} - k_{\max,\sigma}}{k_{i,\sigma}}\right] .$$

Here θ is the angle of incidence at the (ij) interface, $0 \le \alpha \le 1$ depends on the strength of the interface quasiperiodic potential, and the factor c is independent of the emerging layer l. If the roughness in the interface is characterized by more than one typical wave vector, $\mathbf{K}_{ij}$, Eq. (14) can be modified accordingly.

IV. RESULTS

Here results of the MR for $(\mathrm{Fe/Cr})_n$ and $(\mathrm{Fe/Cu})_n$ multilayers with different types of interfaces are presented. In these three metals the isotropic effective mass is assumed to be independent of the material and the spin orientation, with a value of $m_M = m_m = m_S = 4.0 \times$ free-electron mass. With this effective mass the potentials, with respect to the Fermi energy E_F chosen to be at $E_F = 0$, are

$$V_M = -8.23 \text{ eV}, \; V_m = -5.73 \text{ eV for Fe} \; ;$$

$$V_S = -5.77 \text{ eV for Cr} \; ;$$

$$V_S = -8.54 \text{ eV for Cu} \; .$$

Shown in Fig. 2 are MR results for $(\mathrm{Fe/Cr})_n$ superlattices with interfacial scattering given by Eqs. (6) and (11). The MR can vary considerably as a function of η, the magnitude of the geometric roughness, depending on the values of S_σ (i.e., S_M and S_m) in Eq. (11). These results can be understood by examining the plots of the functions of Eq. (11), with $S_\sigma = 1$ and $\eta = 2$ Å shown in Figs. 3 and 4. The electrons transmitted across an interface have the largest asymmetry in the spin-dependent scattering. As seen in Eq. (11) the transmitted portion that is not diffusely scattered, is larger when an electron experiences a small change in potential as it crosses an interface, because the factor in the exponential,

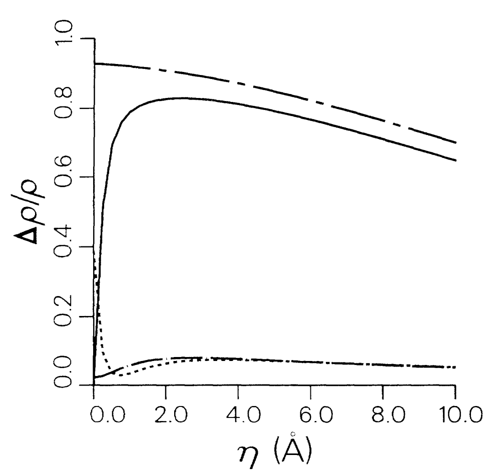

FIG. 2. Variation of $(\Delta\rho/\rho)$ as a function of η, the magnitude of the geometric roughness, for an $(\mathrm{Fe/Cr})_n$ multilayer with interfacial scattering described in Eqs. (6) and (11). The parameters are $d_F = 20$ Å, $d_S = 10$ Å, and $\tau_M = \tau_m = \tau_S = 5 \times 10^{-13}$ sec, with four different values of S_M and S_m: (1) chain-dashed curve $S_M = 0$ and $S_m = 1$; (2) solid curve $S_M = S_m = 1$; (3) dashed curve $S_M = 1$ and $S_m = 0.5$; and (4) chain-dotted curve $S_M = S_m = 0.5$.

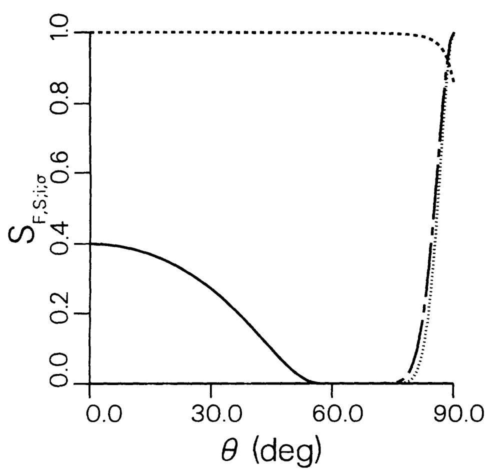

FIG. 3. Variation of $S_{F,S;i;\sigma}$, from Eq. (11), as a function of θ, the angle of incidence, with $S_\sigma=1$ and $\eta=2$ Å for an (Fe/Cr)$_n$ multilayer, with four different values of i and σ: (1) dashed curve $i=S$ and $\sigma=m$; (2) solid curve $i=S$ and $\sigma=M$; (3) chain-dashed curve $i=F$ and $\sigma=m$; and (4) dotted curve $i=F$ and $\sigma=M$. Note that $S_{F,S;S;M}$ is zero for θ greater than the critical angle of incidence; the angle at which $T_{F,S;M}$ goes to zero.

$$(k_{i\sigma}\cos\theta_i - k_{j\sigma}\cos\theta_j)^2 ,$$

is smaller. Since in (Fe/Cr)$_n$

$$|V_M| < |V_S| \approx |V_m| ,$$

the majority electrons are more likely to be diffusely scattered than the minority electrons.

When $S_M=S_m=1$ and $\eta=0$ an electron is always coherently scattered by the potential as it traverses an interface, regardless of the orientation of its spin, and the MR is zero. As η increases the majority-spin electrons are more likely to be diffusely scattered than the minority-spin electrons. As shown in Fig. 2 the MR reaches its maximum value of 82.0% at $\eta\approx2$ Å, which is one-fifth the spacer layer thickness and one-tenth the F layer thickness.

On the other hand, when there is a large asymmetry in the values of S_M and S_m, increasing η from zero lowers the MR, since the net difference in the spin-dependent scattering for the minority and the majority spins will decrease. This can be understood by noting that when η is zero all $S_{j,k;l;\sigma}$ reduce to the angle independent prefactors S_σ of Eq. (11), as shown in Eq. (10). Multiplication of the plots in Figs. 3 and 4, that have $\eta=2$ Å and the prefactors equal to unity, by the constants S_M and S_m where $S_M<1$ and/or $S_m<1$, with S_M very different from S_m, leads to a smaller difference in the spin-dependent scattering for $\eta>0$. This corresponding lowering of the MR with increasing η can be seen in two of the curves ($S_M=0$ and $S_m=1$, and $S_M=1$ and $S_m=0.5$) of Fig. 2. The curve with $S_M=1$ and $S_m=0.5$ falls off more drastically with increasing η because the prefactors S_σ cause the minority spins to be more diffusely scattered, while the exponential or angular dependent part in Eq. (11), shown in Figs. 3 and 4, causes the majority spins for (Fe/Cr)$_n$ to be more diffusely scattered. These two factors cause the asymmetry in the spin-dependent scattering to decrease significantly with increasing η. By contrast the case with $S_M=0$ and $S_m=1$ has a more gradual decrease in the MR with increasing η, because both the prefactors S_σ and the exponentials in Eq. (11) cause the minority-spin electrons to be selectively diffusely scattered so a considerable asymmetry in the spin-dependent interfacial scattering persists.

In general, as a function of η, the MR undergoes the most dramatic changes from $\eta=0$ to $\eta\approx2$ Å. For increasing $\eta>2$ Å the MR falls off gradually. Shown in Figs. 5 and 6 are contour plots of the MR in the parameter space S_M and S_m for (Fe/Cr)$_n$ and (Fe/Cu)$_n$ multilayers. In the region where $S_M\approx S_m$ the MR increases as the geometric roughness η increases from 0 to 2 Å, since the roughness leads to asymmetrical spin-dependent scattering. In the regions where S_M is very different from S_m the MR decreases either slightly or drastically depending on whether the exponentials factors and the constant prefactors S_M and S_m in Eq. (11) lead to a larger or smaller asymmetrical scattering. The region in the parameter space where the MR is the largest for an (Fe/Cu)$_n$ multilayer with $\eta=2$ Å [Fig. 6(b)] is for $S_M>0.75$ and independent of S_m. By contrast, Fig. 5(b) for (Fe/Cr)$_n$ shows that the largest values of the MR occur in the region $S_m>0.65$, independent of S_M. This difference is caused by the different values of the spacer layer potentials for Cu and Cr relative to V_M and V_m for Fe. Since in (Fe/Cu)$_n$

$$|V_M| \approx |V_S| < |V_m| ,$$

the exponential factors in Eq. (11) cause the minority electrons to be diffusely scattered more than the majority

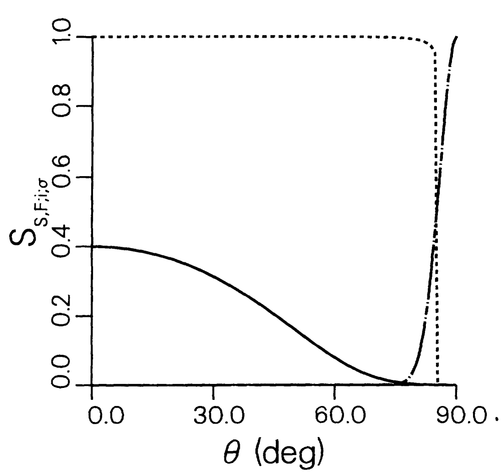

FIG. 4. Variation of $S_{S,F;i;\sigma}$, from Eq. (11), as a function of θ, the angle of incidence, with $S_\sigma=1$ and $\eta=2$ Å for an (Fe/Cr)$_n$ multilayer, with four different values of i and σ: (1) dashed curve $i=F$ and $\sigma=m$; (2) solid curve $i=F$ and $\sigma=M$; (3) chain-dashed curve $i=S$ and $\sigma=m$; and (4) dotted curve $i=S$ and $\sigma=M$. Note that the chain-dashed curve and dotted curve overlap.

electrons. This is opposite to the case of $(Fe/Cr)_n$ mentioned above.

For interfaces with correlated (quasiperiodic) roughness, Eqs. (6), (11), and (14) describe the interfacial scattering. An interface is now characterized by five parameters: S_M, S_m, κ, α, and η. All interfaces in a given multilayer are taken to have the same characteristics; the subscript ij can be dropped from κ_{ij}. Calculations with κ in the range of values satisfying the Bragg condition, i.e., $\kappa \leq 2k_{\max,\sigma}$, where the values of $k_{\max,\sigma}$ depend on the composition of the multilayer, reveal that there are regions of the parameter space S_M, S_m, κ, and η where the MR for $(Fe/Cr)_n$ and $(Fe/Cu)_n$ increases with increasing α.

(1) For $(Fe/Cr)_n$ there are two overlapping regions, called (a) and (b), where the MR increases sharply with increasing α. Increases in the MR, $\Delta \equiv \mathrm{MR}(\alpha=1)-\mathrm{MR}(\alpha=0)$, as large as 61.0% were found.

(2) For $(Fe/Cu)_n$ there is one region, called (c), where the MR increases by moderate amounts. The maximum

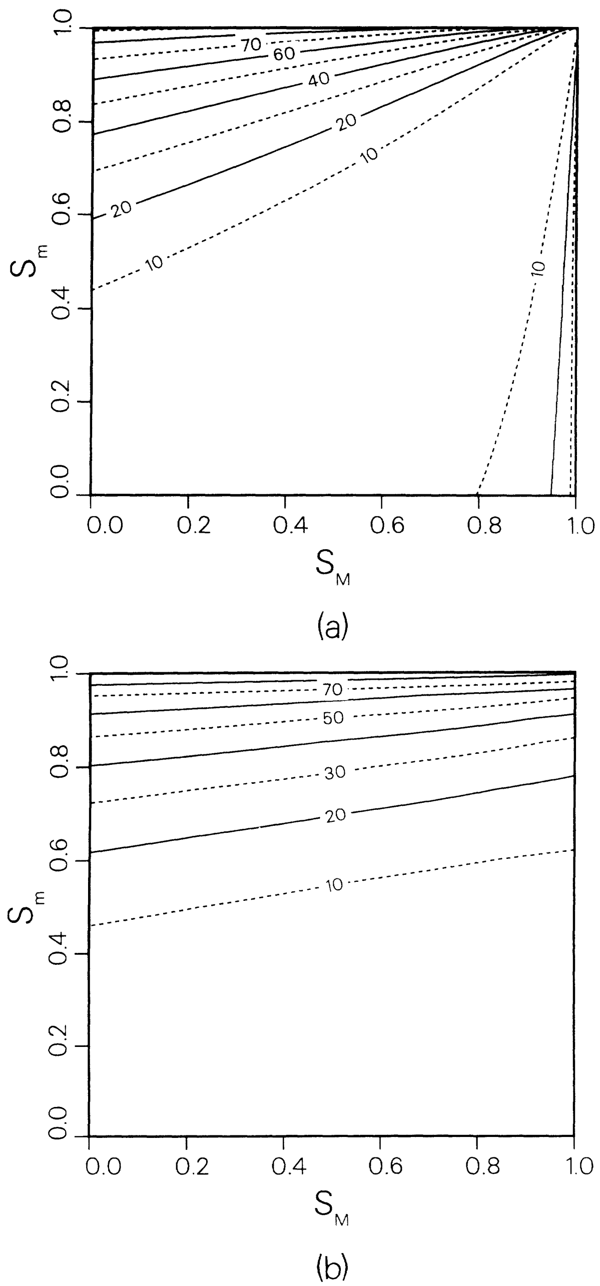

FIG. 5. Contour plots of $\Delta\rho/\rho$ in the parameter space S_m and S_M for an $(Fe/Cr)_n$ multilayer with $d_F=20$ Å, $d_S=10$ Å, $\tau_M=\tau_m=\tau_S=5.0\times10^{-13}$ sec. The electron scattering at the interfaces is described by Eqs. (6) and (11). In (a) $\eta=0$ and in (b) $\eta=2$ Å.

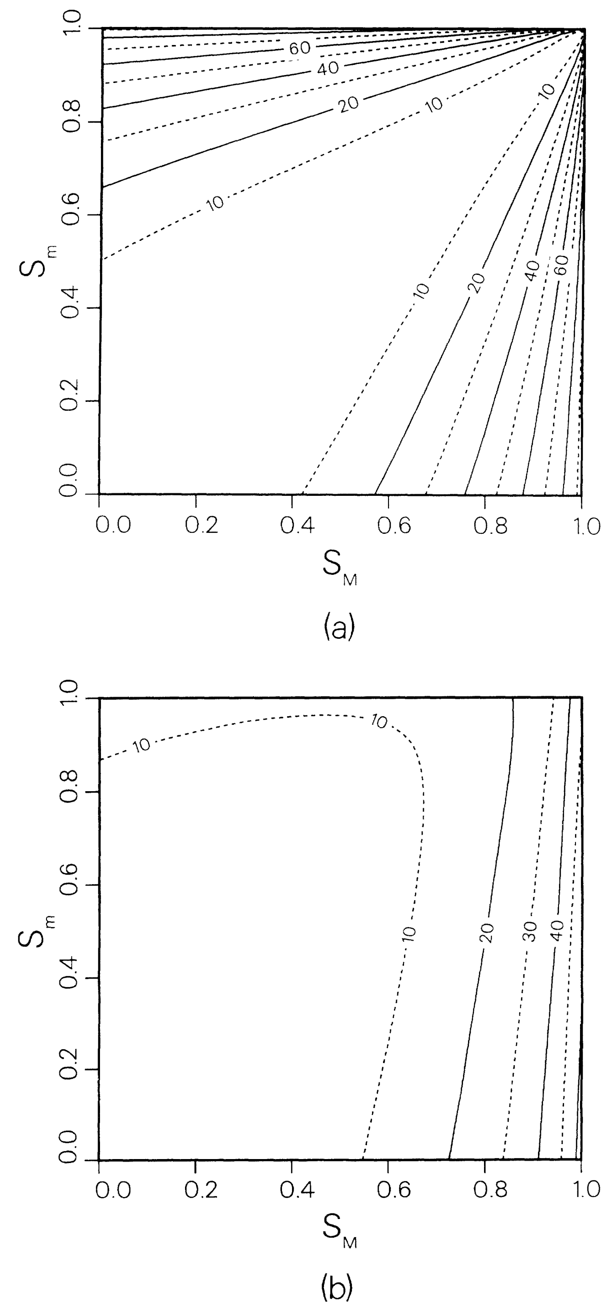

FIG. 6. Contour plots of $\Delta\rho/\rho$ in the parameter space S_m and S_M for an $(Fe/Cu)_n$ multilayer with $d_F=20$ Å, $d_S=10$ Å, $\tau_M=\tau_m=\tau_S=5.0\times10^{-13}$ sec. The scattering at the interfaces is described by Eqs. (6) and (11). In (a) $\eta=0$ and in (b) $\eta=2$ Å.

value of Δ is less than 13.5%. Note that as a function of α, the changes in the MR are always monotonic, in either an abrupt or a gradual manner. In each region there is a set of parameters for which the MR increases the most: In region (a) it is $S_M = S_m = 1$, $\kappa = 4.91$ Å^{-1}, and $\eta = 0$ Å; in region (b) $S_M = 1$, $S_m = 0$, and $\kappa = 5.40$ Å^{-1}, and $\eta = 0$ Å; and in region (c) $S_M = S_m = 1$, $\kappa = 5.92$ Å^{-1}, and $\eta = 2.0$ Å. In all these cases $d_F = 20$ Å, $d_S = 10$ Å, and $\tau_M = \tau_m = \tau_S = 5 \times 10^{-13}$ sec. The reasons for the increase in the MR for these values of the parameters reveal both why the MR increases in these regions and why there is such a marked difference in the magnitude of Δ between $(\mathrm{Fe/Cr})_n$ and $(\mathrm{Fe/Cu})_n$.

For $S_M = S_m = 1$, $\kappa = 4.91$ Å^{-1}, and $\eta = 0$ Å in region (a) the MR is zero when $\alpha = 0$ and 61.0% when $\alpha = 1$. At $\kappa = 4.91$ Å^{-1}, which is identically equal to $k_{F;m} + k_{\max,m}$, the Bragg condition, Eq. (14), is not satisfied by the minority-spin electrons for any angle of incidence on an interface from an F layer to a spacer layer. Since in addition $S_m = 1$, the minority-spin electrons are coherently scattered by the potential on approaching an interface from an F layer. The majority-spin electrons reaching an interface from an F layer with an angle of incidence greater than

$$\theta = \sin^{-1}\left[\frac{4.91\ \text{Å}^{-1} - k_{\max,M}}{k_{F;M}}\right] = 41.4°$$

have a probability α of being diffusely scattered. The asymmetry in the spin-dependent interfacial scattering is the largest when $\kappa = 4.91$ Å^{-1}, $\alpha = 1$ and so is the MR.

The point in region (b) with $S_M = 1$, $S_m = 0$, $\kappa = 5.40$ Å^{-1}, and $\eta = 0$ Å has a MR of 41.1% when $\alpha = 0$ and 90.9% when $\alpha = 1$. The current distribution in the plane of the layers for $\alpha = 0$ and $\alpha = 1$ is shown in Fig. 7. When $\alpha = 0$ the current is largest in the F layers for the spin component in the potential V_M. On the other hand, when $\alpha = 1$ the current of the same spin component in the F layer is considerably reduced. This reduction, which leads to the large increase in MR, can be understood by considering the majority electrons in the F layer incident on an interface. Since $V_M < V_S$ in $(\mathrm{Fe/Cr})_n$ there is a critical angle of incidence $\theta_{c;M}$ such that for larger angles $R_{F,S;M}$ and $T_{F,S;M}$ in Eq. (6) is one and zero, respectively. The critical angle determined from Eqs. (7) and (8) is $\theta_{c;M} = 56.9°$. At $\kappa = 5.40$ Å^{-1}, where the MR is found to increase the most with increasing α,

$$\theta_{c;M} = \sin^{-1}\left[\frac{5.40\ \text{Å}^{-1} - k_{\max,M}}{k_{F;M}}\right] .$$

Since $S_M = 1$, an electron with $\theta_{F,S;M} > \theta_{c;M}$ is totally internally reflected with probability $(1-\alpha)$ and diffusely scattered at the interface with probability α. Therefore, increasing α decreases the amount of current in the F layers for the majority spins both when the magnetic moments of the F layers are in a parallel and in an antiparallel configuration. The electrons with $\theta_{F,S;M} < \theta_{c;M}$ have a nonzero probability $T_{F,S;M}$ of being transmitted into the spacer layer. When the magnetic moments of the F

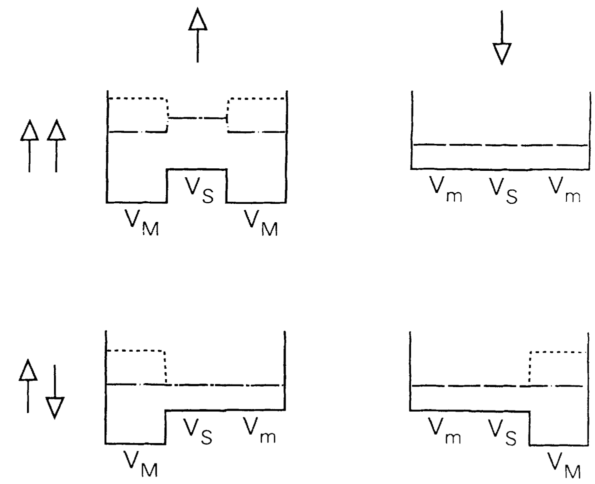

FIG. 7. Diagrams of the potentials and the calculated in-plane current $J_x(z)$ for the $\uparrow$-spin and $\downarrow$-spin electrons in the parallel ($\uparrow\uparrow$) and in the antiparallel ($\uparrow\downarrow$) configurations of an $(\mathrm{Fe/Cr})_n$ multilayer in which three of the layers are shown. The scattering at the interfaces is described by Eqs. (6), (11), and (14) where $S_M = 1$, $S_m = 0$, $\eta = 0$, and $\kappa = 5.404$ Å^{-1}, with two different values of α: (1) dashed curve $\alpha = 0$; and (2) chain-dotted curve $\alpha = 1$. The other parameters are $d_F = 20$ Å, $d_S = 10$ Å, and $\tau_M = \tau_m = \tau_S = 5.0 \times 10^{-13}$ sec.

layers are parallel these electrons are not diffusely scattered at any interface, but are always diffusely scattered at alternating interfaces when the F layers are antiparallel, since $S_m = 0$. In short increasing α removes the portion of electrons in the F layers that are totally internally reflected, i.e., channeled. These electrons make an equal contribution to the conductivity for the F layers in a parallel $\sigma\uparrow\uparrow$ and in an antiparallel $\sigma\uparrow\downarrow$ configuration. By removing this equal contribution the remaining unequal contributions to the conductivities in Eq. (1), mainly arising from $S_m = 0$, become more pronounced, causing an increase in the MR.

At the point $S_M = S_m = 1$, $\kappa = 5.92$ Å^{-1}, and $\eta = 2.0$ Å in region (c) for $(\mathrm{Fe/Cu})_n$ the MR increases from 48.2 to 61.5 % as α increases from 0 to 1. The increase is the result of the interplay between the scattering due to the geometric roughness, Eq. (11), and the quasiperiodic roughness, Eq. (14), which tend to produce the largest spin-dependent asymmetry for those electrons near normal incidence and grazing incidence, respectively.

In contrast to $(\mathrm{Fe/Cr})_n$, where there are two substantial regions, (a) and (b), in parameter space where Δ is large, in $(\mathrm{Fe/Cu})_n$ there is only a small region (c) where the MR increases moderately with increasing α. The reason is that $V_S < V_M$. To illustrate this point we discuss two sets of values of the parameters for $(\mathrm{Fe/Cu})_n$ that are analogous to those analyzed for $(\mathrm{Fe/Cr})_n$ in regions (a) and (b). If we consider the MR as a function of α for different values of κ with $S_M = S_m = 1$ and $\eta = 0$, similar to the point considered in region (a) for $(\mathrm{Fe/Cr})_n$, we find no value of κ such that only one spin component is selectively diffusely scattered at an interface. For instance if κ is chosen so as to maximize the interfacial diffuse scattering of the majority-spin electrons from the Fe layer without affecting the minority-spin electrons, the electrons in the Cu spacer layer impinging on an interface are still diffusely scattered because $k_s > k_{F;M}$ at the Fermi energy. This lack of asymmetry in the total spin-dependent scattering at the interfaces prevents the MR from increasing as a function of α. When $\alpha=0$ the point in parameter space with $S_M=1$, $S_m=0$, and $\eta=0$, similar to the point considered in region (b) for $(Fe/Cr)_n$, has a larger contribution to the current in the Cu layers than in the Fe layers. The larger current in the Cu layer occurs only when the magnetic moments of the F layers are parallel and only for the spin component that experiences the potential V_M in the F layers. The larger current is caused by channeled electrons in the Cu layers that are nondiffusively scattered, since $S_M=1$, and totally internally reflected for angles of incidence greater than a critical angle, since $V_S < V_M$. This channeled current leads to a larger MR, since it contributes to $\sigma\uparrow\uparrow$ but not to $\sigma\uparrow\downarrow$. For κ in a range of values that destroys this channeled current the MR will decrease with increasing α, unlike the increase that occurs in $(Fe/Cr)_n$, since the channeling that is destroyed there occurs in the F layers when the magnetic moments are both parallel and antiparallel.

V. CONCLUSIONS

In studying the influence of interface scattering on the negative magnetoresistance of ferromagnetic–normal-metal multilayers, three aspects have been considered: (1) random geometric roughness described by η, the mean-square deviation of the interfaces from being atomically flat, (2) correlated (quasiperiodic) roughness, characterized by the dominant $\mathbf{k}$ vector of the coherence κ, and the scattering strength α, and (3) averaged effects due to impurities, interdiffusion, band structure, etc. The last effect has been included in a simple way using the parameters S_M and S_m. Geometric uncorrelated roughness scatters electrons at normal incidence more efficiently, while the correlated (quasiperiodic) roughness has its greatest effect on electrons at grazing angles. These different properties of the interfaces can combine to produce either a large or a small asymmetry in the spin-dependent interfacial scattering. A giant MR results whenever the spin asymmetry is large. Further experimental and theoretical investigations are needed to ascertain which properties of the interfaces are realized during fabrication of multilayers by means of various techniques.

ACKNOWLEDGMENTS

This research was supported, at the Lawrence Berkeley Laboratory, by the Director, Office of Energy Research, Office of Basic Energy Sciences, Materials Sciences Division, U.S. Department of Energy, under Contract No. DE-AC03-76SF00098.

[1] G. Binasch, P. Grünberg, F. Saurenbach, and W. Zinn, Phys. Rev. B **39**, 4828 (1989).
[2] B. Dieny, V. S. Speriosu, S. S. P. Parkin, B. A. Gurney, D. R. Wilhoit, and D. Mauri, Phys. Rev. B **43**, 1297 (1991).
[3] A. Chaiken, P. Lubitz, J. J. Krebs, G. A. Prinz, and M. Z. Harford, J. Appl. Phys. **70**, 5864 (1991).
[4] B. Dieny, V. S. Speriosu, S. Metin, S. S. P. Parkin, B. A. Gurney, P. Baumgart, and D. R. Wilhoit, J. Appl. Phys. **69**, 4774 (1991).
[5] A. Chaiken, T. M. Tritt, D. J. Gillespie, J. J. Krebs, P. Lubitz, M. Z. Harford, and G. A. Prinz, J. Appl. Phys. **69**, 4798 (1991).
[6] A. Chaiken, G. A. Prinz, and J. J. Krebs, J. Appl. Phys. **67**, 4892 (1990).
[7] T. Miyazaki, T. Yaoi, and S. Ishio, J. Magn. Magn. Mater. **98**, L7 (1991).
[8] M. N. Baibich, J. M. Broto, A. Fert, F. Nguyen Van Dau, F. Petroff, P. Etienne, G. Creuzet, A. Friederich, and J. Chazelas, Phys. Rev. Lett. **61**, 2472 (1988).
[9] S. S. P. Parkin, N. Moore, and K. P. Roche, Phys. Rev. Lett. **64**, 2304 (1990).
[10] S. S. P. Parkin, Z. G. Li, and D. J. Smith, Appl. Phys. Lett. **58**, 2710 (1991).
[11] F. Petroff, A. Barthélémy, D. H. Mosca, D. K. Lottis, A. Fert, P. A. Schroeder, W. P. Pratt, Jr., and R. Loloee, Phys. Rev. B **44**, 5355 (1991).
[12] W. P. Pratt, Jr., S. F. Lee, J. M. Slaughter, R. Loloee, P. A. Schroeder, and J. Bass, Phys. Rev. Lett. **66**, 3060 (1991).
[13] P. Baumgart, B. A. Gurney, D. R. Wilhoit, T. Nguyen, B. Dieny, and V. Speriosu, J. Appl. Phys. **69**, 4792 (1991).
[14] S. S. P. Parkin, Appl. Phys. Lett. **61**, 1358 (1992).
[15] E. E. Fullerton, D. M. Kelly, J. Guimpel, I. K. Schuller, and Y. Bruynseraede, Phys. Rev. Lett. **68**, 859 (1992).
[16] R. Q. Hood and L. M. Falicov, Phys. Rev. B **46**, 8297 (1992).
[17] R. E. Camley and J. Barnaś, Phys. Rev. Lett. **63**, 664 (1989).
[18] J. Barnaś, A. Fuss, R. E. Camley, P. Grümberg, and W. Zinn, Phys. Rev. B **42**, 8110 (1990).
[19] P. M. Levy, S. Zhang, and A. Fert, Phys. Rev. Lett. **65**, 1643 (1990); S. Zhang, P. M. Levy, and A. Fert, Phys. Rev. B **45**, 8689 (1992).
[20] J. Inoue, A. Oguri, and A. Maekawa, J. Phys. Soc. Jpn. **60**, 376 (1991).
[21] K. Fuchs, Proc. Cambridge Philos. Soc. **34**, 100 (1938).
[22] E. H. Sondheimer, Adv. Phys. **1**, 1 (1952).
[23] E. C. Stoner, Proc. R. Soc. London Ser. A **165**, 372 (1938).
[24] A. Fert and I. A. Campbell, J. Phys. F **6**, 849 (1976); I. A. Campbell and A. Fert, in *Ferromagnetic Materials*, edited by E. P. Wohlfarth (North-Holland, Amsterdam, 1982), Vol. 3, p. 769.
[25] The boundary conditions (5) correspond to the situation discussed in BA, Ref. 16, of complete specular reflection at the outer surfaces, $P=1$.
[26] S. B. Soffer, J. Appl. Phys. **38**, 1710 (1967).
[27] V. Bezák and J. Krempaský, Czech. J. Phys. B **18**, 1264

(1968).

[28]V. Bezák, M. Kedro, and A. Pevala, Thin Solid Films **23**, 305 (1974).

[29]P. Beckmann and A. Spizzichino, *The Scattering of Electromagnetic Waves from Rough Surfaces* (Pergamon, Oxford, 1963), pp. 70–98.

[30]It should be noted that the derivation of the equations in Refs. 26–29 require a correlation length longer than the electron Fermi wavelength, so that a vector normal to the surface can be properly defined. In this sense the limit $L \rightarrow 0$ is not strictly valid. It should be understood as the limit in which L is still longer than the Fermi wavelength but shorter than all other lengths in the problem.

[31]If the geometric random roughness of the interfaces were the only source of scattering, the prefactors in Eq. (11) must all be taken to be $S_\sigma = 1$. This is, however, not a realistic assumption. Impurities and other defects at the interfaces scatter electrons of opposite spin in a different way. Hence S_M and S_m are not equal, and in general both less than one.

[32]It should be emphasized that "roughness" with a single, given periodicity, produces Bragg beams with well-defined directions of propagation, i.e., electron trajectories with their own (positive or negative) contribution to the current. For a smooth, nonuniform, quasiperiodic distribution of geometrical defects at the interface (i.e., a Fourier transform of the topography consisting of a peaked but continuous function), the distribution of velocities of electrons Bragg scattered over the Fermi surface tends to average down to zero, resulting in the electrons being effectively removed from the current-carrying distribution, i.e., relaxing back to equilibrium.

[33]As in Eq. (7), the masses $m_{i\sigma}$ and $m_{j\sigma}$ in Eq. (12) are assumed to be equal. All calculations presented in the paper have $m_{i\sigma} = m$, independent of the layer i and the spin σ.